# 3D X-RAY CT IMAGING OF THE BONE LACUNO-CANALICULAR NETWORK

*Françoise Peyrin[1,2], Alexandra Pacureanu[1,2], Maria Alejandra Zuluaga[1,2], Pei Dong[1,2], Max Langer[1]*

[1] CREATIS, Inserm, U1044; CNRS, UMR5220; INSA-Lyon;
Université de Lyon; Université Lyon 1 ; F-69621, Villeurbanne, France
[2] ESRF, Imaging Group, 38043 Grenoble Cedex

## ABSTRACT

Imaging of the trabecular bone network has made significant advances in the last decade thanks to the outstanding development of 3D X-ray micro-CT. Compared to standard histomorphometry, this technique provides non-destructively 3D images of the trabecular bone permitting a so-called model-independent quantification of this network. Today, the assessment of the bone Lacuno-Canalicular Network (LCN) is a new challenge at the cellular scale. The LCN forms a communication network interconnecting the osteocytes, the bone cells embedded in the mineralized matrix. It plays a major role in mechanotransduction with important implications on bone remodeling and finally bone strength. However, methods for the 3D assessment of the LCN are lacking. In a recent work, we have shown the feasibility of imaging the LCN in 3D thanks to Synchrotron Radiation nano-CT (voxel size 280 nm). These first images of the LCN in 3D open new challenges in image processing to segment and quantify the LCN. After recalling the principle of image acquisition, we present our first approaches for enhancing the contrast of canaliculi and segmenting the LCN. Finally, to increase the connectivity of the network, we consider a new approach based on 3D geodesic voting, offering promising perspectives. Results on experimental 3D images of the 3D LCN in human femoral bone are presented.

***Index Terms***— X-ray CT, micro-CT, nano-CT, synchrotron radiation, bone micro-architecture, osteocyte network

## 1. INTRODUCTION

Osteoporosis is a frequent bone fragility disease in the elderly with important consequences in terms of quality of life. Since the occurrence of the disease is increasing with the ageing of the population, it represents a serious public health problem [1]. Osteoporosis is associated to an increase risk of fractures, more frequently at the hip or at the spine. The diagnosis of osteoporosis currently relies on dual X-ray absorptiometry (DXA) to assess bone mineral density (BMD). However while BMD traduces bone mass, it is not sufficient to explain the risk of fracture, and factors of bone quality should be considered. These factors include the micro organization of bone and the material properties of bone tissue.

Bone has a hierarchical organization from the macro to the nanoscale At the microstructural level, two types of bones can be considered: cortical bone is dense while trabecular bone is a highly porous network made of a complex arrangement of thin trabeculae ( mean thickness ~ 100-150µm). The investigation of trabecular bone micro-architecture received a lot of attention during the last decade. While the gold standard was histomorphometry, based on the microscopic analysis of thin bone slice, the development of X-ray micro-CT has permitted to image this network in 3D and non-destructively [2]. For quantification, the neat advantage of 3D images, is the possibility to extract direct 3D parameters characterizing the network [3]. Conversely to histomorphometry parameters, derived by assuming that the trabecular bone follows a parallel-plate model, 3D direct parameters do not rely on any model and are thus more reliable. 3D X-ray micro-CT is also a tool of choice to analyze cortical bone which is another determinant of bone strength. Cortical porosity constitutes a complex network made of Haversian and Volkman canals, but the analysis of its 3D organization has so far received less attention [4].

At the cellular level, another major network of interest is the lacuno-canalicular network (LCN) which will be the focus of this paper. The LCN encompasses the osteocyte system which has recently been recognized to play a key role in sensing and responding to mechanical stimuli [5] [6]. The osteocytes are the most numerous bone cells communicating through dendritic processes. The LCN is thus composed of osteocyte lacunae (size of a few µm) linked with each other through thin channels (diameter ~100-700 nm) called canaliculi. While this system raises increasing attention, it is poorly known due to the lack of investigation techniques. Till now, reported characteristics of the LCN are based on optical or electronical 2D microscopic observations [7]. A recent review has highlighted the need and the lack of 3D assessment techniques of the LCN network [8]. The nanoscale dimensions of the LCN and its location, deeply embedded in bone tissue, explains the difficult in its investigation.

The techniques reported so far for imaging the LCN in 3D were confocal microscopy [9], focus ion beam (FIB) [10], and ptychography [11]. While confocal microscopy is the most widespread, its use to image the LCN is quite restricted and it suffers from a lack of spatial resolution in the depth direction making quantification difficult. FIB is a destructive technique and acquisition time in ptychography remains prohibitive for applications. In addition, these techniques were only demonstrated on less than one to two cells which does not properly allow speaking of a network.

We recently showed the feasibility of imaging the LCN by parallel-beam Synchrotron Radiation (SR) CT at the nanoscale [12]. This provided the first 3D images of the LCN with a voxel size 280 nm and over a large field of view (~ 500 µm). These first images of the LCN in 3D open new challenges in image processing to segment and quantify the LCN. Due to the limited spatial resolution compared to the canaliculi size, and photonic noise, the segmentation of the LCN is particularly challenging.

In this paper, after recalling the principle of image acquisition, we present our first approaches for enhancing the contrast of canaliculi and segmenting the LCN based on a level set approach. Finally, to increase the connectivity of the network, we investigate a novel approach based on 3D geodesic voting, offering promising perspectives. The methods are illustrated on experimental 3D images of the LCN in human femoral bone.

## 2. 3D SR NANO-CT IMAGE ACQUISITION

SR nano-CT was performed on the 3D parallel beam setup developed on beamline ID19 at the ESRF *[13][14]*. Briefly, synchrotron sources permits to use monochromatic X-ray beams with flux several orders of magnitude higher than that of conventional X-ray sources. These properties allow to increase the signal to noise ratio (SNR) and to avoid beamhardening artifacts. A series of 2D radiographs of the sample are acquired on a 2D detector composed of a scintillator, converting X-ray photons into visible light, light microscope optics for magnification and a CCD camera. Thanks to different optical systems, the pixel size on the detector can be set between 30 µm down to 170nm.

A voxel size of 300nm was selected to image the LCN. However the first experiments did not allow to discriminate canaliculi. The optimization of the setup was necessary to ensure canaliculi visibility. X-ray dose exposure should be kept as low as possible to avoid motion artifacts due to radiation damage. A decisive element was found to be the scintillator which should be efficient while maintaining a sufficient spatial resolution, which are antagonist properties. Experiments with different scintillators coupled to two different CCD cameras allowed to select a 6µm-thick GGG scintillator associated to a E2V CCD camera. 2000 projections were acquired with an exposure time of 0.3s. The CT image was then reconstructed by 3D filtered backprojection. A typical 2D slice in a human femoral bone sample is illustrated in Figure 1. Osteocyte lacunae can be recognized as the larger black ellipses while canaliculi are difficult to see since they appear as very small struts corresponding to the intersection of canaliculi with the sectioning plane.

## 3. IMAGE SEGMENTATION

The reduced contrast and signal to noise ratio of the images, as well as the limited size of the canaliculi make the latter prone to partial volume effects, challenging their segmentation. To this aim, we first describe a segmentation method based on line- contrast enhancement.

### 3.1. Enhancement of canaliculi

Hessian-based filters have primarily been proposed to enhance vessels in medical images from different modalities such as MRI or angiography [15] [16]. The Hessian matrix which describes the second-order structure of the local intensity variations contains shape information about the objects in the image. The mutual relationships between its eigenvalues correspond to the geometrical properties of the local structure.

Let $f(\mathbf{x})$ with $\mathbf{x}=(x,y,z)$ be the 3D image. To reduce the effect of noise, the second derivative were calculated after smoothing with a Gaussian kernel $g_\sigma(\mathbf{x})$ as:

$$f_{ab}(\mathbf{x};\sigma)=\left\{\frac{\partial^2}{\partial a\partial b}g_\sigma(\mathbf{x})\right\}*f(\mathbf{x}) \qquad (1)$$

where *a,b* are the row and column indices in the Hessian matrix. Let $|\lambda_1|\le|\lambda_2|\le|\lambda_3|$ be the eigenvalues of the Hessian matrix at voxel **x**. A voxel in an ideal tubular structure should be characterized by: $|\lambda_1|\approx 0$ ; $|\lambda_1|<<|\lambda_2|$ and $|\lambda_2|\approx|\lambda_3|$. Sato used two of the eigenvalues to compute a similarity measure [15] and Frangi et al. [16] proposed a criterion based on all the three eigenvalues.

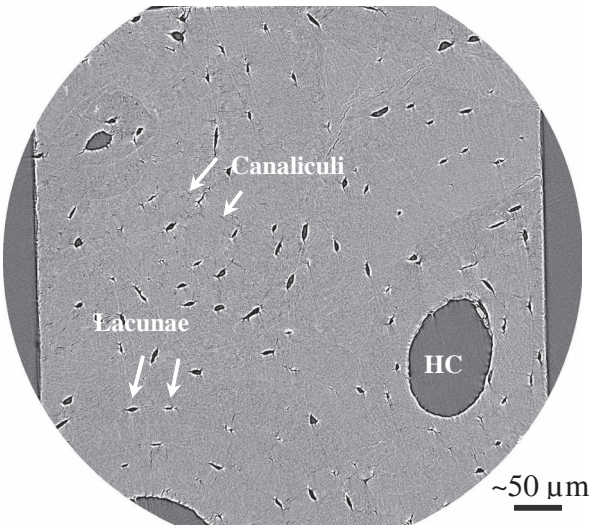



**Fig 1** SR nano-CT slice from a human femoral cortical bone sample. Around the Haversian canals (HC), osteons are formed from concentrical lamellae interspersed with osteocytes in lacunae interconnected through canaliculi.

The line filters as defined by Sato or Frangi permit to enhance curvilinear features, but they are not sufficient to extract the LCN. Due to their ellipsoidal shape, the lacunae are removed from the filtered image. Moreover, the filter transforms the noise from the original image into a structured background noise. This is due, on one hand, to the fact that the bone matrix doesn't appear homogeneous at this spatial resolution. In addition, the size of canaliculi is in the range of the high frequencies, requiring to tune the filter to detect very fine features, creating opportunities to detect line-like paths formed by the noise.

We proposed a non-linear filtering method inspired from bilateral filters [17], to combine the 3D line filter map with the original grey-level image. Conversely to linear filters, the kernel is not fixed, but it updates for each image element as function of the local 3D line filter response. If $l(\mathbf{x})$ is the 3D line-filter map, the proposed non-linear filter is $f_{NL}(\mathbf{x})$:

$$f_{NL}(\mathbf{x})=\frac{1}{Z}\sum_{\mathbf{x}'\in W_{\mathbf{x}}}f(\mathbf{x}')\exp\left(-\frac{1}{2}\left(\frac{l(\mathbf{x})-l(\mathbf{x}')}{\sigma_W}\right)^2\right) \qquad (2)$$

with $$Z=\sum_{\mathbf{x}'\in W_x}\exp\left(-\frac{1}{2}\left(\frac{l(\mathbf{x})-l(\mathbf{x}')}{\sigma_W}\right)^2\right) \qquad (3)$$

where $W_{\mathbf{x}}$ is a neighborhood of $\mathbf{x}$, and $\sigma_W$ is the standard deviation which enables to tune the selectivity of the filter. This permits to smooth the background without affecting the sharpness of the canaliculi and the cell lacunae are reconstructed. Figure 2c) illustrates a 3D rendering of the result of this non-linear filtering applied to a subvolume of the 3D image.

### 3.2. Level-set based segmentation

From the image resulting of the application of the non-linear filter described in the previous section, a rough segmentation can be obtained by simple thresholding. However, the connectivity of the LCN is not well preserved.

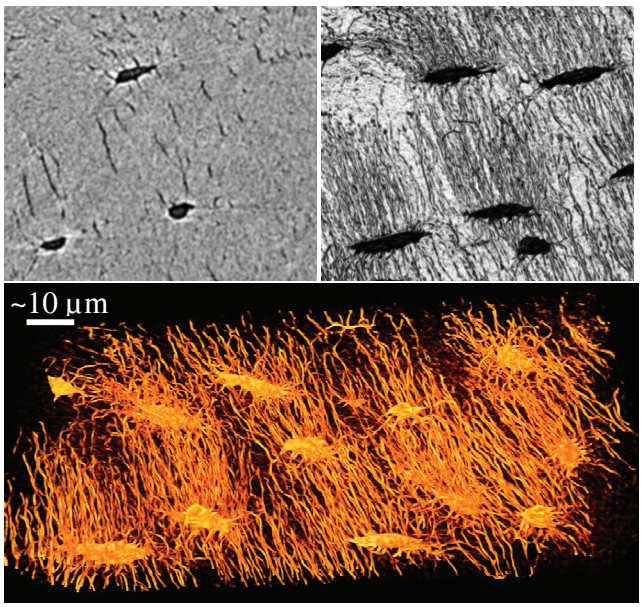



**Fig 2** a) portion of original SR µCT slice b) MIP (Maximum of Intensity) rendering c) 3D rendering of the non-linear line enhancement filtered image

In order to cope with this problem, we investigated a method based on level-sets. The evolution of the level method is determined by a speed function, which was chosen following the approach proposed by Caselles and Sethian [18]. The speed term includes an image term, a regularization based on mean curvature, and an advection term.

Level-set results showed an important sensitivity of the method to initialization. The only feasible way to obtain satisfying results was to initialize the method with a selective pre-segmentation. Since each image contain thousands of cell lacunae and hundreds of thousands of canaliculi, a fast and automatic initialization method was necessary. The aim of our initialization was to put a germ in each cell and each canaliculi. It was based on the result of the non-linear line enhancement filter, which was thresholded by maximizing the inter-class entropy. To remove residual noise, erosion with a structuring element of radius 1 was performed. Then, the propagation of the level-set was based on fast marching [19]. The method was implemented by using the ITK library (Kitware®). The various parameters regulating the level set segmentation were selected after systematic testing on a realistic phantom. This phantom was obtained by semi-manual segmentation on a sub-volume selected from an experimental image.

At the end of the process, a connected component analysis was performed. The individual components smaller than a certain size, were filtered in order to remove small residues belonging to the bone matrix.

A quantitative evaluation of the whole method was performed based on the realistic phantom testing the sensitivity, specificity and the connectivity degree of the results.

Figure 3 shows a 3D rendering of the segmented image obtained with this method. This display reveals the circular arrangement of the osteoctye lacunae around the Haversian canal and the density and the high complexity of the canaliculi.

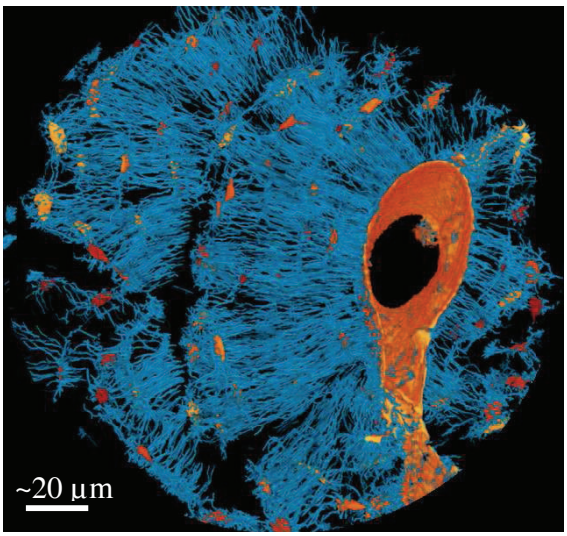



**Fig 3 :** Level-set segmentation of the LCN. (blue : canaliculi, orange and red : cell lacunae and the Haversian canal). The lacunae have been separately segmented in order to facilitate visualization.

### 3.3. 3D geodesic voting

An alternative to overcome the discontinuity problem is to use a minimum cost path approach. Minimal paths search to find a connected path between two user-provided start and end points in a cost image, minimizing the total cost of the path. They are well known to guarantee that the global minimum is found, thus avoiding early stopping. Moreover, they are not as computationally expensive. Their sole drawback is that they require the input of start and end points that are typically provided manually, which can be tedious when many branches are to be extracted.

We build up on the seminal geodesic voting idea of Rouchdy and Cohen [20] to construct a LCN segmentation framework. We seek to exploit the advantages of the minimum cost path techniques while reducing the necessity of user interaction. Our aim is to connect the lacunae (start points) with the canaliculi extremities (end points) so that the extracted path allows us to obtain continuous segmented canaliculi.

Obtaining the set A of start points is rather simple. Lacunae can be roughly segmented through simple thresholding. The gravity centers of the segmented structures were used as A points. On the other hand, the selection of end points is more complex as it is difficult to establish the location of the canaliculi extremities. Given a set of end random points dispersed in the image, Rouchdy and Cohen [20] proposed a geodesic voting scheme that allows the extraction of minimal paths without having information about the location of the B set. The method propagates a front in an image using the Fast Marching algorithm [19] starting from a set of user-provided start points. Then back-propagation is used to extract minimal paths, $y$, that connect end points in B to the start points in A. The geodesic voting at voxel $\mathbf{p}$ of the image is defined by:

$$G(\mathbf{p}) = \sum_{k=1}^{N} \delta_{\mathbf{p}}(y_k) \qquad (4)$$

where $\delta_p(y) = 1$ if the path $y$ crosses the voxel $\mathbf{p}$ and 0 otherwise. Voxels with a high geodesic voting score G, are kept while the others are rejected.

As our images are volumetric, we have extended the original 2D voting formulation so that it can be applied on 3D data. The implementation of geodesic voting requires to define a scheme to select the B set. Rouchdy and Cohen [20] suggested the use of points randomly distributed within the image or regularly distributed along the image boundary. Whereas the former approach is computationally expensive, the latter leads into the so-called shading problem, i.e. some zones obtain a null voting score although there are branches that should be extracted. To avoid this problem, we chose to tackle each lacuna separately (instead of processing the image as a whole) by defining a volume of interest (VOI) that surrounds each lacuna. The VOI borders build up the B set for a particular lacuna. The process of partitioning the image into subvolumes containing one and only one lacuna is called lacuna tessellation.

The feasibility of the method was demonstrated on subvolumes from the 3D experimental data. Fig. 4 illustrates the obtained results, showing a good detection and connectivity of the extracted network The results were obtained using the response of a vesselness filter [15] as an input for the Fast Marching algorithm

.

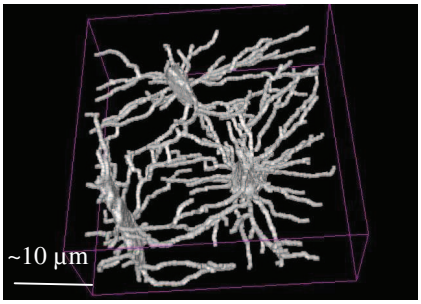



Fig 4. Segmented sub-volume containing 3 connected lacunae.

## 5. CONCLUSION

Although the bone LCN is raising increasing interest, there is a lack of assessment techniques. We demonstrated the feasibility of SR nano-CT to image the LCN in 3D. However, these unprecedented images are demanding in terms of image analysis.

A non-linear line-enhancement filter was proposed to enhance the contrast of canaliculi. Different segmentation methods, such as simple thresholding and level sets were then tested. They were useful to provide 3D renderings of the LCN. Nevertheless, a close examination of the images shows a lack of continuity in some areas due to partial volume effect. Thus a method able to improve the connectivity of the network was sought for. To this aim, a minimal path approach was investigated. The originality is to propose an automatic placement of seeds conversely to the methods developed so far, and to implement the process in 3D. The segmentation of canaliculi associated to several osteocyte lacunae showed a good connectivity. The main restriction of the method remains computing time to process large images $(2048)^3$ containing up to 1000 cells. To solve this problem, parallel computing solutions will be investigated. After segmentation, new methods for the quantification of the LCN will be developed.

In conclusion, this technique opens remarkable perspectives for the three-dimensional evaluation of the bone cell network. With adapted developments in image analysis, it is promising to provide for the first time, quantitative data on bone physiopathology at the cellular scale.

## 7. REFERENCES


[1] O. Johnell and J. A. Kanis, "An estimate of the worldwide prevalence and disability associated with osteoporotic fractures," *Osteoporos Int*, vol. 17, no. 12, pp. 1726-1733, Dec. 2006.

[2] Feldkamp, L.A. and Goldstein, S.A.; Parfitt, A.M.; Jesion, G. & Kleerekoper, M., "The direct examination of three-dimensional bone architecture in vitro by computed tomography," *J. Bone Miner. Res.*, vol. 4, pp. 3-11, 1989.

[3] Hildebrand, T. & Rüegsegger, P., "A new method for the model independentassessment of thickness in three-dimensionalimages," *J. Microsc.*, no. 185, pp. 67-75, 1997.

[4] V. Bousson, F. Peyrin, C. Bergot, M. Hausard, A. Sautet, and J. D. Laredo, "Cortical bone of the human femoral neck : three-dimensional appearance and porosity using synchrotron radiation," *J Bone Min Research*, vol. 19, no. 5, pp. 794-801, 2004.

[5] E. H. Burger and J. Klein-Nulend, "Mechanotransduction in bone - role of the lacuno-canalicular network," *FASEB J.*, vol. 13, no. 9001, pp. 101-112, May 1999.

[6] L. F. Bonewald, "The amazing osteocyte," *J Bone Miner Res*, vol. 26, no. 2, pp. 229-238, Feb. 2011.

[7] G. Marotti, M. Ferretti, F. Remaggi, and C. Palumbo, "Quantitative evaluation on osteocyte canalicular density in human secondary osteons," *Bone*, vol. 16, no. 1, pp. 125-128, Jan. 1995.

[8] P. Schneider, M. Meier, R. Wepf, and R. Müller, "Towards quantitative 3D imaging of the osteocyte lacuno-canalicular network," *Bone*, vol. 47, no. 5, pp. 848-858, Nov. 2010.

[9] Y. Sugawara, H. Kamioka, T. Honjo, K.-ichi Tezuka, and T. Takano-Yamamoto, "Three-dimensional reconstruction of chick calvarial osteocytes and their cell processes using confocal microscopy," *Bone*, vol. 36, no. 5, pp. 877-83, May 2005.

[10] P. Schneider, M. Meier, R. Wepf, and R. Müller, "Serial FIB/SEM imaging for quantitative 3D assessment of the osteocyte lacuno-canalicular network," *Bone*, vol. 49, no. 2, pp. 304-311, Aug. 2011.

[11] M. Dierolf, A. Menzel, P. Thibault, P. Schneider, C. M. Kewish, R. Wepf, O. Bunk, and F. Pfeiffer, "Ptychographic X-ray computed tomography at the nanoscale," *Nature*, vol. 467, no. 7314, pp. 436-439, Sep. 2010.

[12] A. Pacureanu, M Langer, E Boller, P Tafforeau, Paul, and F Peyrin, , "Nanoscale imaging of the bone cell network with synchrotron X-ray tomography," sub *Med Phys*, 2011.

[13] M. Salomé, F. Peyrin, P. Cloetens, C. Odet, A. M. Laval-Jeantet, J. Baruchel, and P. Spanne, "A synchrotron radiation microtomography system for the analysis of trabecular bone samples," *Med Phys*, vol. 26, no. 10, pp. 2194-2204, Oct. 1999.

[14] T. Weitkamp, P. Tafforeau, E. Boller, P. Cloetens, J.-P. Valade, P. Bernard, F. Peyrin, W. Ludwig, L. Helfen, and J. Baruchel, "Status and evolution of the ESRF beamline ID19," *AIP Conf. Proc.*, vol. 1221, no. 1, pp. 33-38, Apr. 2010.

[15] Y. Sato, S. Nakajima, N. Shiraga, H. Atsumi, S. Yoshida, T. Koller, G. Gerig, and R. Kikinis, "Three-dimensional multi-scale line filter for segmentation and visualization of curvilinear structures in medical images," *Med Image Anal*, vol. 2, no. 2, pp. 143-168,. 1998.

[16] A. Frangi, W. Niessen, K. Vincken, and M. Viergever, "Multiscale Vessel Enhancement Filtering," in *Medical Image Computing and Computer-Assisted Interventation — MICCAI'98*, 1998, p. 130.

[17] C. Tomasi and R. Manduchi, "Bilateral filtering for gray and color images," presented at the Sixth International Conference on Computer Vision, 1998, 1998, pp. 839-846.

[18] V. Caselles, R. Kimmel, and G. Sapiro, "Geodesic active contours," Los Alamitos, CA, USA, 1995, vol. 0, p. 694.

[19] J. A. Sethian, "A Fast Marching Level Set Method for Monotonically Advancing Fronts," *PROC. NAT. ACAD. SCI*, vol. 93, p. 1591--1595, 1995.

[20] Y. Rouchdy and L. D. Cohen, "Image segmentation by geodesic voting. Application to the extraction of tree structures from confocal microscope images," ICPR 2008, 2008, pp. 1-5.